DNA Photocleavage by Phenanthrenequinone Diimine Complexes of Rhodium(III): Shape-Selective Recognition and Reaction

Ayesha Sitlani, Eric C. Long,† Anna M. Pyle,‡ and Jacqueline K. Barton*

Contribution from the Division of Chemistry and Chemical Engineering, California Institute of Technology, Pasadena, California 91125. *Received July 10, 1991*

Abstract: $Rh(phen)_2phi^{3+}$ and $Rh(phi)_2bpy^{3+}$ (phi = 9,10-phenanthrenequinone diimine, phen = 1,10-phenanthroline, bpy = 2,2′-bipyridyl) bind double helical DNA avidly ($K \geq 10^7\ M^{-1}$) by intercalation and with photoactivation promote strand cleavage. $Rh(phen)_2phi^{3+}$ and $Rh(phi)_2bpy^{3+}$ unwind double helical DNA by 21° and 18°, respectively, per bound complex. The quantum yields for nucleic acid base release at 313 nm are 0.0012 for $Rh(phen)_2phi^{3+}$ and 0.0003 for $Rh(phi)_2bpy^{3+}$. While both complexes have similar photochemical properties, overall binding modes and affinities, their cleavage patterns, observed on ^{32}P-end-labeled DNA restriction fragments and oligonucleotide substrates, indicate substantially different recognition characteristics. $Rh(phen)_2phi^{3+}$ binds DNA with some sequence selectivity, preferring 5′-pyrimidine-pyrimidine-purine-3′ sites and cleaving with 5′-asymmetry, while $Rh(phi)_2bpy^{3+}$ binds in a predominantly sequence-neutral fashion. These differences in recognition characteristics may be understood based upon the different shapes of the complexes. Owing to steric interactions of the ancillary phenanthroline ligands, $Rh(phen)_2phi^{3+}$ appears to bind preferentially to sites which are more open in the major groove; since no similar steric constraints arise with an ancillary phi ligand, $Rh(phi)_2bpy^{3+}$ binds all sites with similar affinities. The shapes of these complexes also govern their chemistry of strand scission. Chemical modification studies and HPLC analyses of the DNA termini and monomeric products formed in the $Rh(phi)^{3+}$ induced DNA cleavage reactions have been conducted to characterize the products formed upon photoreaction of the rhodium complexes with 5′-CTGGCATGCCAG-3′. For $Rh(phen)_2phi^{3+}$, the primary products are oligomers containing 3′- and 5′-phosphate termini and nucleic acid bases (in stoichiometric proportion). For $Rh(phi)_2bpy^{3+}$, these same products account for approximately 70% of the reaction, but in addition base propenoic acids and a terminus assigned as a 3′-phosphoglycaldehyde are obtained in a correlated amount (30% of reaction). The formation of base propenoic acids and 3′-phosphoglycaldehydes are found furthermore to depend upon oxygen concentration, while other products are oxygen-independent. *The products obtained are consistent with photoreaction of $Rh(phi)^{3+}$, intercalated in the major groove of DNA, via abstraction of a C3′–H atom of the deoxyribose.* Subsequent addition of dioxygen to the C3′–H radical or solvation would lead to the degradation products obtained. The partitioning between the oxygen dependent and independent pathways of DNA strand scission is found to correlate best with how the shape of the complex limits access of dioxygen to the C-3′ position. While $Rh(phi)_2bpy^{3+}$ was found to promote the oxygen-dependent pathway to an extent of approximately 30%, $Rh(phen)_2phi^{3+}$, with ancillary phenanthrolines that overhang and shelter the C3′-position, appears to disfavor this pathway of DNA degradation. These studies underscore the importance of shape-selection in governing not only recognition but also reaction of molecules on the helix. Such an intimate relationship between recognition and reaction of molecules bound selectively to DNA requires consideration in understanding the reactions of DNA-binding proteins and small molecules.

Introduction

During the past decade there has been increasing attention devoted to the study and development of novel molecules which recognize DNA sites and induce strand scission.[1-4] While most small molecular weight natural products bind to DNA in the minor groove of the helix,[2-4] our laboratory has been interested in the design of transition metal complexes which target DNA sites in the major groove.[1] The study of such agents may be useful in the design of novel chemotherapeutics and tools for biotechnology. Such developments require an increased understanding of those factors governing binding and recognition of DNA by both small molecules and proteins. Recently, our laboratory has reported[5] a new class of DNA binding agents based on phenanthrenequinone diimine complexes of rhodium(III). Bis(phenanthroline)(9,10-phenanthrenequinone diimine)rhodium(III) [$Rh(phen)_2phi^{3+}$] and bis(9,10-phenanthrenequinone diimine)(bipyridyl)rhodium(III) [$Rh(phi)_2bpy^{3+}$] were found to induce efficient nucleic acid strand scission in the presence of long wavelength UV light.[5] These complexes, while exhibiting similar cleavage properties and products, were found to display vastly different DNA recognition properties owing to subtle differences in their individual shapes. $Rh(phen)_2phi^{3+}$ was found to display marked sequence selectivity with a general preference for 5′-pyrimidine(py)-pyrimidine-purine(pu)-3′ steps. In comparison $Rh(phi)_2bpy^{3+}$ preferred 5′-pu-py-pu-3′ steps and induced DNA strand scission in a predominantly sequence neutral fashion. These results underscore the importance of *shape-selection* in the targeting of small molecules to DNA.[1e,5]

$Rh(phen)_2phi^{3+}$ appears to target the DNA major groove as do DNA-binding proteins.[6] Owing to shape-selection, the rhodium complex furthermore can provide a structural probe of the major groove. Recent work has shown that enantiomers of $Rh(phen)_2phi^{3+}$ distinguish DNA sites on the basis of the shape and asymmetry associated with propeller twisting.[7] In addition to

* Author to whom correspondence should be addressed.
† Present address: Department of Chemistry, Purdue University School of Science, Indiana University—Purdue University at Indianapolis, Indianapolis, IN 46205.
‡ Present address: Department of Chemistry and Biochemistry, University of Colorado, Boulder, CO 80309.

(1) (a) Barton, J. K. *Science* **1986**, *233*, 727. (b) Fleisher, M. B.; Mei, H.-Y.; Barton, J. K. *Nucleic Acids Mol. Biol.* **1988**, *2*, 65. (c) Kirshenbaum, M. R.; Tribolet, R.; Barton, J. K. *Nucl. Acids Res.* **1988**, *16*, 7983. (d) Mei, H.-Y.; Barton, J. K. *Proc. Natl. Acad. Sci. U.S.A.* **1988**, *85*, 1339. (e) Barton, J. K.; Pyle, A. M. *Prog. Inorg. Chem.* **1990**, *38*, 413.
(2) (a) Dervan, P. B. *Science* **1986**, *232*, 464. (b) Moser, H. E.; Dervan, P. B. *Science* **1987**, *238*, 645. (c) Sigman, D. S. *Acc. Chem. Res.* **1986**, *19*, 180. (d) Metal-DNA Chemistry; ACS Symposium Series 402; Tullius, T. D., Ed.; American Chemical Society: Washington, DC, 1989.
(3) Stubbe, J.; Kozarich, J. W. *Chem. Rev.* **1987**, *87*, 1107.
(4) (a) Hecht, S. M. *Acc. Chem. Res.* **1986**, *19*, 383. (b) Zein, N.; Sinha, A. M.; McGarhren, W. J.; Ellestad, G. A. *Science* **1988**, *240*, 1198. (c) Kappen, L. S.; Goldberg, I. H.; Wu, S. H.; Stubbe, J.; Worth, L., Jr.; Kozarich, J. W. *J. Am. Chem. Soc.* **1990**, *112*, 2797. (d) Gale, E. F.; Cundliffe, E.; Reynolds, P. E.; Richmond, M. H.; Waring, M. J. *The Molecular Basis of Antibiotic Action*; Wiley: London, 1981.
(5) (a) Pyle, A. M.; Long, E. C.; Barton, J. K. *J. Am. Chem. Soc.* **1989**, *111*, 4520. (b) Pyle, A. M. Ph.D. Thesis, Columbia University, 1989.
(6) (a) Steitz, T. A. *Q. Rev. Biophys.* **1990**, *23*, 205. (b) Harrison, S. C.; Aggarwal, A. K. *Annu. Rev. Biochem.* **1990**, *59*, 933.

0002-7863/92/1514-2303$03.00/0

Chart I

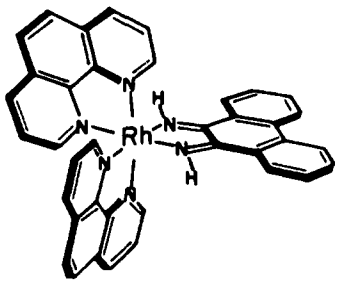

$Rh(phen)_2(phi)^{3+}$

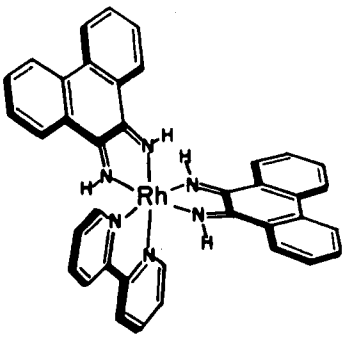

$Rh(phi)_2(bpy)^{3+}$

recognizing structural microheterogeneities of the DNA helix, $Rh(phen)_2phi^{3+}$ has also been shown to recognize regions that exhibit tertiary interactions, such as the triply bonded sites on tRNA molecules.[8] $Rh(phen)_2phi^{3+}$ has also been useful in delineating structural features of the binding site for the transcription factor TFIIIA,[9] further suggesting that DNA-binding proteins may recognize DNA sites through considerations of shape in addition to the direct readout of hydrogen bonds. In a complementary fashion, $Rh(phi)_2bpy^{3+}$, owing to its sequence-neutrality, serves as a novel photofootprinting reagent for proteins and small molecules which bind to DNA.[10] Exploitation of the different DNA recognition properties of $Rh(phen)_2phi^{3+}$ and $Rh(phi)_2bpy^{3+}$ has, therefore, allowed the development of both a highly selective probe of nucleic acid structure and a sequence-neutral cleavage agent.

Here we describe in detail the DNA binding, site recognition, and cleavage products exhibited by $Rh(phi)^{3+}$ complexes and show how the differences in the individual shapes of these molecules affect both their DNA recognition characteristics and their chemistry of strand scission. These findings illustrate a unique relationship between shape-selective recognition and the mechanism of DNA cleavage.

Experimental Section

Materials. Calf thymus DNA was purchased from Sigma. Topoisomerase I was purchased from BRL, and plasmid pUC18 was purchased from Boeringer-Mannheim. Phosphoramidites and solid supports for oligonucleotide synthesis were obtained from Pharmacia. $[Rh(phen)_2(phi)]Cl_3$ and $[Rh(phi)_2(bpy)]Cl_3$ were synthesized as described previously.[11] All enzymes utilized were from commercial sources. [α-^{32}P]dideoxy-ATP and [γ-^{32}P]ATP were obtained from Amersham and NEN-Dupont, respectively.

Instrumentation. The light source utilized in all cleavage experiments was an Oriel Model 6140 1000 W Hg/Xe lamp fitted with a monochromator and a 300-nm cut-off filter to avoid light damage to the DNA. Absorption spectra were recorded on a Cary 219 spectrophotometer. High performance liquid chromatography (HPLC) was performed on a Waters 600E system equipped with a 484 tunable detector. Autoradiograms were scanned with a LKB 2202 Ultrascan Laser Densitometer.

Topoisomerase-Mediated Unwinding of Plasmid DNA. Measurements of helical unwinding by the rhodium complexes were performed using topoisomerase I as described earlier for the analogous ruthenium complexes.[12]

Absorption Titrations and Equilibrium Dialysis Measurements of Binding to DNA. Equilibrium dialysis measurements were performed as described previously for ruthenium complexes.[12] Absorption titrations were performed by monitoring the changes in the absorbance spectra of the metal complex (3–10 μM Rh^{3+}) in buffer (50 mM NaCl, 5 mM tris, pH 7.5) in the presence of increasing amounts of DNA (5–40 μM DNA in nucleotides).

Determination of Quantum Yields. Measurements of the quantum yield of nucleic acid base release was performed on 2.0-mL aqueous solutions containing 300 or 500 μM (nucleotide) calf thymus DNA and 30 μM $Rh(phen)_2phi^{3+}$ or $Rh(phi)_2bpy^{3+}$ in 25 mM sodium cacodylate buffer, pH 7.0. The solutions were stirred vigorously while irradiated at 313 nm for timed intervals (0, 60, 90, and 120 min for $Rh(phen)_2phi^{3+}$ and 180 and 330 min for $Rh(phi)_2bpy^{3+}$) followed by examination of 25-μL reaction aliquots by HPLC in order to quantitate nucleic acid base release. The quantum yields were calculated as described previously[11] where moles reaction product per time are defined as moles of nucleic acid base released per time, and the moles photons absorbed per time was determined as a photon flux of 4.18×10^{-7} Ein/min.

Photocleavage of a DNA Restriction Fragment. Supercoiled pUC18 plasmid was digested with HindIII restriction endonuclease followed by treatment with calf intestinal alkaline phosphatase. Separate batches of digested plasmid were either 3′-end-labeled by treatment with terminal deoxynucleotidyl transferase and [α-^{32}P]-dideoxy-ATP or 5′-end-labeled with T4 polynucleotide kinase and [γ-^{32}P]-ATP.[13] After labeling, the DNA was digested with PvuII to yield a 90 and 230 base pair fragment. The 90 base pair fragment was purified by 6% preparative nondenaturing gel electrophoresis and isolated by electroelution.

Cleavage reactions were carried out in 20-μL volumes contained in 0.65-mL siliconized eppendorf tubes. The reaction mixtures were prepared with 50 μM (nucleotide) calf thymus DNA containing labeled restriction fragment and 5 μM rhodium in 50 mM sodium cacodylate buffer, pH 7.0. Reaction mixtures containing $Rh(phen)_2phi^{3+}$ were irradiated for 1 min at 356 nm, while those containing $Rh(phi)_2bpy^{3+}$ were irradiated for 4 min at 313 nm. Controls without metal complex were also irradiated in parallel to test for light damage.

After irradiation, all reaction mixtures were ethanol precipitated with the addition of 10 μL of 7.5 M NH_4OAc and 90 μL of EtOH. The precipitated DNA was dried and resuspended in 3 μL of 80% formamide loading buffer (80% v/v deionized formamide, 50 mM tris-borate, pH 8.3, 1 mM EDTA, 0.1 w/v xylene cyanol, 0.1% w/v bromophenol blue). All rhodium reactions along with Maxam-Gilbert G+A sequencing reactions[13] were heat denatured at 90 °C and quick-chilled on ice. The samples were loaded onto a 12% (19:1) polyacrylamide/7.5 M urea sequencing gel. Gels were electrophoresed at 1700 V for approximately 4 h and transferred to a cassette and stored at −70 °C with Kodak X-Omat film.

Photocleavage of Oligonucleotides. All oligonucleotides utilized during the course of study were synthesized on a Pharmacia Gene Assembler using the phosphoramidite method and purified by reverse-phase HPLC. Oligonucleotides were 5′- or [3′-^{32}P]-end-labeled using T4 polynucleotide kinase and [γ-^{32}P]ATP or terminal deoxytransferase and [α-^{32}P]dideoxy-ATP, respectively.[13] The end-labeled oligonucleotides were subjected to photocleavage in a 40 μL total volume containing 0.5 mM (nucleotide) of the oligonucleotide substrate, 50 mM sodium cacodylate buffer, pH 7.0, and 25 μM metal complex. Samples were irradiated with a 1000 W Hg/Xe lamp at 310 nm for 7.5 min. Samples containing typically 25 000 cpm ^{32}P were resuspended in loading dye, loaded onto a 20% denaturing polyacrylamide sequencing gel, and electrophoresed at 1700 V for approximately 4 h. Autoradiography was performed using Kodak X-Omat film followed by densitometric analysis.

(7) Pyle, A. M.; Morii, T.; Barton, J. K. *J. Am. Chem. Soc.* **1990**, *112*, 9432.
(8) Chow, C. S.; Barton, J. K. *J. Am. Chem. Soc.* **1990**, *112*, 2839.
(9) Huber, P.; Morii, T.; Mei, H.-Y.; Barton, J. K. *Proc. Natl. Acad. Sci. U.S.A.* **1991**, *88*, 10801.
(10) Uchida, K.; Pyle, A. M.; Morii, T.; Barton, J. K. *Nucl. Acids Res.* **1989**, *17*, 10259.
(11) Pyle, A. M.; Chiang, M.; Barton, J. K. *Inorg. Chem.* **1990**, *29*, 4487.
(12) Pyle, A. M.; Rehmann, J. P.; Meshoyrer, R.; Kumar, C. V.; Turro, N. J.; Barton, J. K. *J. Am. Chem. Soc.* **1989**, *111*, 3051.
(13) Maniatis, T.; Fritsch, E. F.; Sambrook, J. *Molecular Cloning*; Cold Spring Harbor Laboratory, 1982.

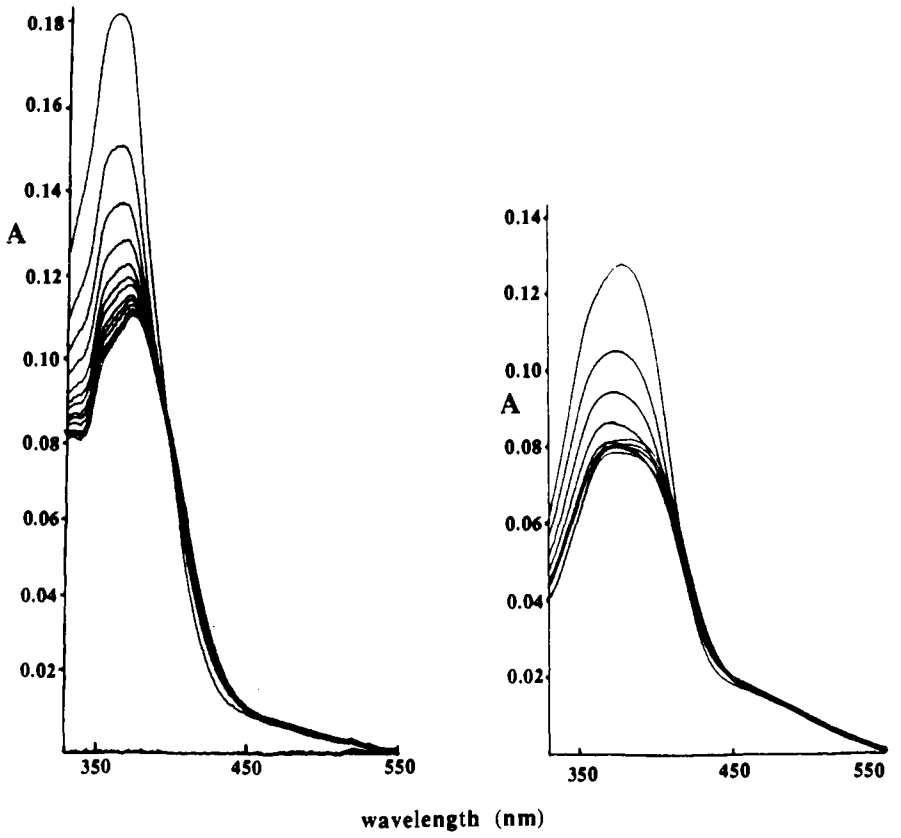

Figure 1. Absorbance hypochromism of Rh(phen)$_2$phi^{3+} (left) and Rh(phi)$_2$bpy^{3+} (right) upon addition of calf thymus DNA. The absorbance of each Rh complex was monitored as a function of increasing DNA (nucleotide) concentration. (Left panel) 9.9 μM Rh(phen)$_2$phi^{3+} in the presence of 0, 39, 58, 77, 86, 95, 104, 113, 122, 131, 140, 148, and 157 μM nucleotides resulting in increasing absorbance hypochromism: λ_{max} of free Rh(phen)$_2$phi^{3+}, 360 nm; λ_{max} of DNA-bound Rh(phen)$_2$phi^{3+}, 376 nm (16 nm red shift); hypochromicity, 42.3%. (Right panel) 11.4 μM Rh(phi)$_2$bpy^{3+} in the presence of 0, 15, 30, 44, 58, 72, 86, 100, 113, and 127 μM nucleotides resulting in increasing absorbance hypochromism: λ_{max} of free Rh(phi)$_2$bpy^{3+}, 381 nm; λ_{max} of DNA-bound Rh(phi)$_2$bpy^{3+}, 392 nm (11 nm red shift); hypochromicity, 31%.

In order to determine the effects of neutral, alkaline, and reductive conditions on photocleavage products, a single photocleavage reaction in a 40-μL reaction volume was divided into 3 aliquots and treated as follows. (i) *Neutral*: 10 μL photocleavage reaction was lyophilized and resuspended in loading buffer. (ii) *Alkaline*: 10 μL reaction mixture was brought to a final NaOH concentration of 0.1 M and incubated at 60 °C for 2 min. The reaction was quenched with HCl, lyophilized to dryness, and then resuspended in loading buffer. (iii) *$NaBH_4$ treatment*: 10-μL reaction was brought to a final $NaBH_4$ concentration of 0.3 M and incubated at 0 °C for 90 min. The sample was then quenched with HCl, lyophilized to dryness, and resuspended in loading buffer. All the samples resuspended in loading dye were then heat denatured at 90 °C for 2 min and loaded onto a 20% polyacrylamide gel. Alternatively, to detect the presence of metastable intermediates, the heat treatment was avoided, and the samples were directly loaded onto a 20% polyacrylamide gel.

Cleavage of Oligonucleotides under Conditions of Varying Oxygen Concentration. Cleavage reactions contained 500 μM (nucleotide) 5′-$C_1T_2G_3G_4C_5A_6T_7G_8C_9C_{10}A_{11}G_{12}$-3′ with [5′-^{32}P]-end-labeled material and 25 μM final concentration metal complex in 50 mM sodium cacodylate, pH 7.0, 40 μL total volume. Reaction mixtures were contained in a quartz tube with a septum; they were either purged with dioxygen or argon through a narrow gauge needle or maintained under ambient conditions during the course of sample irradiation (7.5 min at 310 nm). After irradiation the reaction mixtures were dried and resuspended in loading buffer. Reaction aliquots were then heat denatured at 90 °C for 2 min and examined by 20% polyacrylamide gel electrophoresis, as described above.

Densitometry and Data Analysis. Densitometry was performed directly on autoradiograms produced from polyacrylamide gels. Methods for densitometry and data collection have all been described previously.[10]

Quantitative Cleavage of Oligonucleotide Substrates and Determination of Base Products Released. Typically, nucleic acid base release from oligonucleotide substrates was examined after irradiation (310 nm for 7.5 min) of a reaction volume of 40 μL containing 0.5 mM (nucleotide) of the oligonucleotide and 25 μM metal complex in 50 mM sodium cacodylate buffer, pH 7.0 (differences from this standard procedure are noted in Table III). Quantitation of nucleic acid base release was performed on a Cosmosil 5 μ, 15-cm C-18 column washed with 0.5 M ammonium formate at a flow rate of 1.5 mL min^{-1}. Products were detected by UV absorbance at 260 nm and quantitated by comparison of peak areas generated with commercial standards. Quantitation of the extent of oligonucleotide digested for comparison to nucleic acid base release was made on a Cosmosil 5 μ, 15-cm C-18 column washed with 0.1 M ammonium formate using a 0–20% linear CH_3CN gradient. Nucleic acid base products were detected at 260 nm. Adenine, thymine, guanine, and cytosine were eluted with retention times of 13.0, 5.7, 4.4, and 2.0 min, respectively, while the base propenoic acids had a retention time of 1.4 min.

Table I. Summary of DNA Binding and Spectral Parameters of Rh(phen)$_2$phi^{3+} and Rh(phi)$_2$bpy^{3+}

metal complex	unwinding angle (deg)	hypochromism[a] (%)	red shift[b] (nm)
Rh(phen)$_2$phi^{3+}	21	42 (360 nm)	16
Rh(phi)$_2$bpy^{3+}	18	31 (381 nm)	11

[a] Absorbance hypochromism at the wavelength of maximum absorbance for free complex. [b] Red shift in the absorbance maximum in the presence of DNA.

Results

DNA Binding and Helix Unwinding by Rhodium Complexes. Several different assays were employed to determine the extent of binding of the Rh(phi)$^{3+}$ complexes to DNA. The results of absorption titrations are shown in Figure 1. The phi-centered $\pi \rightarrow \pi^*$ transitions of both Rh(phen)$_2$phi^{3+} and Rh(phi)$_2$bpy^{3+} are strongly affected by binding to DNA, resulting in substantial hypochromism and shifts to longer wavelengths of the phi-centered transition (Table I). Isosbestic points are evident at 391 nm for Rh(phen)$_2$phi^{3+} and at 406 and 458 nm for Rh(phi)$_2$bpy^{3+}. However, an accurate determination of the binding constants of the rhodium complexes to DNA could not be made from absorption titrations since essentially stoichiometric binding was evident at micromolar concentrations. For the same reason,

Scheme I[a]

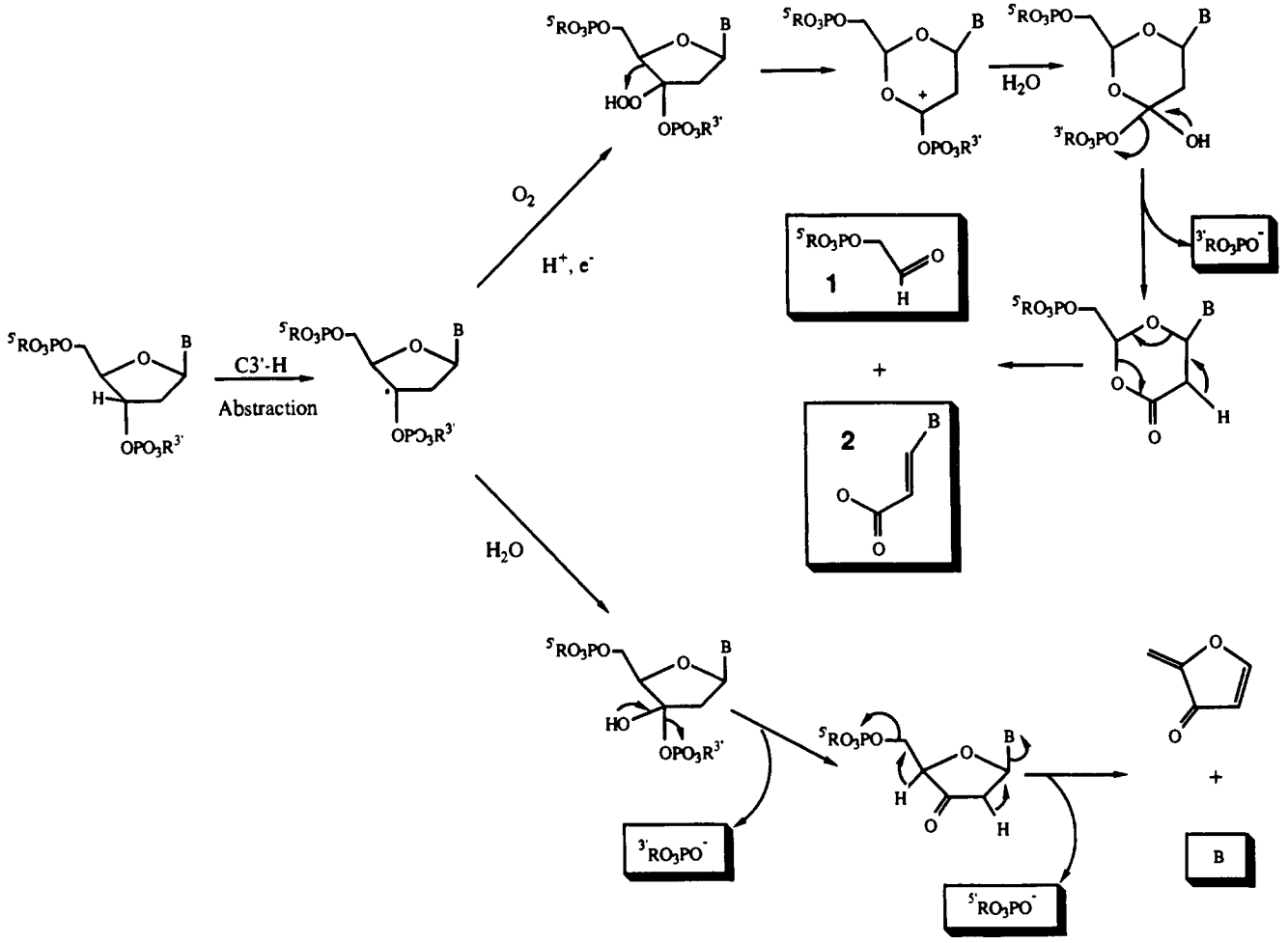

[a] This scheme has been adapted from ref 3. The products identified after photocleavage by the metal complexes are highlighted (boxed).

equilibrium dialysis measurements (data not shown) were unreliable at values of bound metal/nucleotide ratios of less than 0.7. In comparison to the binding studies, cleavage experiments showed that the complexes readily induce DNA strand scission at concentrations as low as 0.1 μM. Therefore, based on the above data, it is reasonable to make an estimate of $K_B \geq 10^7$ M^{-1} as the lower limit of DNA binding for $Rh(phi)^{3+}$ complexes. As reported previously,[10] the competitive footprinting studies with distamycin also yielded a minimum binding constant for $Rh(phi)_2bpy^{3+}$ of 10^7 M^{-1} for low affinity sites.

Like their ruthenium(II) analogues,[12] $Rh(phen)_2phi^{3+}$ and $Rh(phi)_2bpy^{3+}$ also readily unwind superhelical DNA. The circular plasmid pBR322 was treated with topoisomerase in the presence of varying concentrations of rhodium, and after removal of the rhodium complex (by ethanol precipitation) the number of supercoils restored were counted. Given a binding constant of 10^7 M^{-1}, we can assume full binding of the rhodium complex to the helix at concentrations of rhodium of 0.1 to 0.5 μM. On this basis, the unwinding per rhodium bound can be determined. As given in Table I, the topoisomerase assay showed that $Rh(phen)_2phi^{3+}$ and $Rh(phi)_2bpy^{3+}$ unwinds DNA by 21° and 18°, respectively. These values are comparable to those found with other intercalating agents.[14]

Site-Selectivities on DNA Restriction Fragments and Oligonucleotides. Both $Rh(phen)_2phi^{3+}$ and $Rh(phi)_2bpy^{3+}$ promote DNA strand cleavage upon photoactivation and with comparable quantum efficiencies. For $Rh(phen)_2phi^{3+}$ and $Rh(phi)_2bpy^{3+}$ the quantum efficiencies for nucleic acid–base release are 12×10^{-4} and 2.8×10^{-4}, respectively, at 313 nm. This compares closely to the quantum efficiencies of 27×10^{-4} and 2.1×10^{-4} for photoanation at 313 nm of $Rh(phen)_2phi^{3+}$ and $Rh(phi)_2bpy^{3+}$, respectively.[11] As shown previously, $Rh(phen)_2phi^{3+}$ promotes DNA cleavage with site-selectivity, while $Rh(phi)_2bpy^{3+}$ appears more sequence-neutral in terms of its recognition properties. This is evident in Figure 2A. Cleavage is seen with $Rh(phi)_2bpy^{3+}$ at all sites on the [5'-^{32}P]-end-labeled restriction fragment, whereas a few preferred sites of cleavage are apparent with $Rh(phen)_2phi^{3+}$. In this experiment comparable concentrations and irradiation times have been employed; therefore, the differences in cleavage may be seen to reflect differences in the recognition properties of the complexes.

The sequence-selective nature of $Rh(phen)_2phi^{3+}$ can be examined in the histogram shown in Figure 2B. Inspection of this figure indicates that the preferred sites of cleavage for this complex are contained within a 5'-py-*py*-pu-pu-3' site with cleavage occurring directly at the highlighted residue. Although the sequence 5'-CCAG-3' shows the highest levels of cleavage, there is a marked level of cleavage at similar sequences such as 5'-CCAA-3'. Significant levels of induced strand scission also occur at sequences such as 5'-T*T*GG-3', 5'-T*T*AA-3', and to a lesser extent at other sites containing a central 5'-py-pu-3' site. Figure 2B also illustrates that cleavage of these sequences is associated with an additional cleavage site located at the pyrimidine residue of the complementary strand resulting in a 5'-asymmetric cleavage pattern. This 5'-asymmetry is evident reproducibly also on oligonucleotides of different sequence[7,15] and on several different restriction fragments.[5] The observed 5'-asymmetry is usually separated by one nucleotide, although two nucleotide shifts and occasionally no shift (cleavage directly across from the pyrimidine residue) is observed. Figure 2B also illustrates that along with a preference for 5'-

(14) Neidle, S.; Abraham, Z. *CRC Crit. Rev. Biochem.* **1984**, *17*, 73.

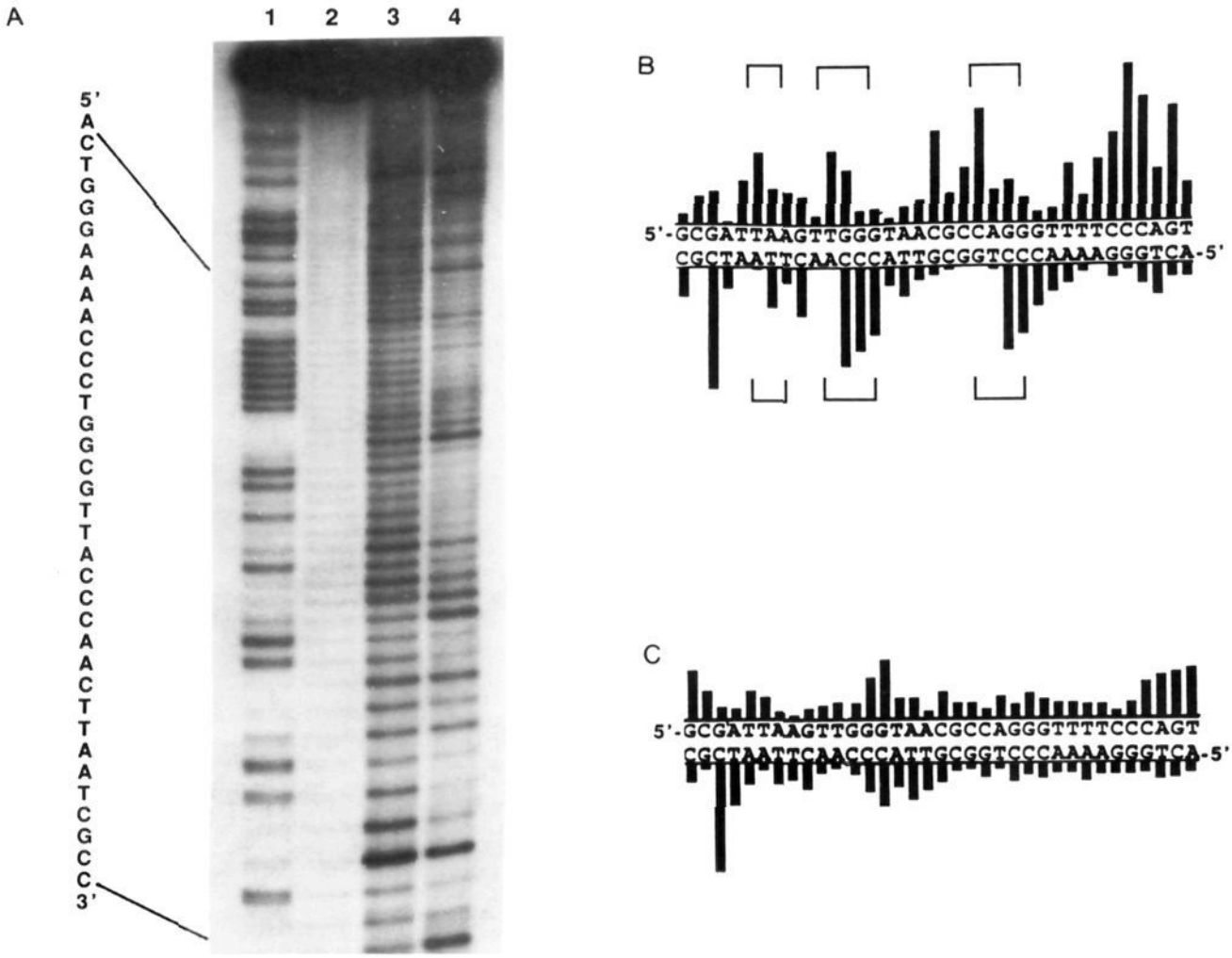

Figure 2. Comparison of Rh(phen)$_2$phi^{3+} and Rh(phi)$_2$phi^{3+} photocleavage. A. Autoradiogram of a polyacrylamide gel after photocleavage of a [3′-^{32}P]-end-labeled restriction fragment: lane 1, Maxam–Gilbert G + A reaction; lane 2, light control irradiated in the absence of metal complex; lane 3, fragment irradiated in the presence of Rh(phi)$_2$bpy^{3+}; lane 4, fragment irradiated in the presence of Rh(phen)$_2$phi^{3+}. Reaction conditions are given in the Experimental Section. B. Histogram illustrating the relative cleavage by Rh(phen)$_2$phi^{3+} at sites along the 5′-end-labeled fragment (top) and the 3′-end-labeled fragment (bottom). C. Histogram illustrating the relative cleavage by Rh(phi)$_2$bpy^{3+} at sites along the 5′-end-labeled fragment (top) and the 3′-end-labeled fragment (bottom).

py-*py*-pu-3′ sites, Rh(phen)$_2$phi^{3+} shows some preference for homopyrimidine stretches.

In contrast to Rh(phen)$_2$phi^{3+}, Rh(phi)$_2$bpy^{3+} is less selective for particular DNA sites. The histogram (Figure 2C) reveals a comparable extent of cleavage at all sites. However, the photocleavage patterns do show some preference for sites 5′-ATCG-3′, 5′-ACCA-3′, and 5′-CCCA-3′, all of which contain a central 5′-*py*-py-3′. In comparison, cleavage experiments on other restriction fragments[5,10] have demonstrated that Rh(phi)$_2$bpy^{3+} shows an overall preference for 5′-pu-*py*-pu-py-3′ stretches, in particular the 5′-A*T*GC-3′ site, with cleavage occurring at the highlighted pyrimidine.

As illustrated in Figure 3, similar recognition patterns for the complexes are also observed when the oligonucleotide 5′-CTGGCATGCCAG-3′ is utilized as a substrate. As expected, Rh(phi)$_2$bpy^{3+} cleaves strongly at the T$_7$ of the 5′-pu-*py*-pu-py-3′ site and moderately at the C$_9$ of the 5′-G$_8$C$_9$C$_{10}$A$_{11}$-3′ (5′-pu-*py*-py-3′) site. Rh(phen)$_2$phi^{3+} cleaves most strongly at C$_{10}$ (5′-C$_9$C$_{10}$A$_{11}$G$_{12}$-3′) and targets the alternating 5′-pu-*py*-pu-py-3′ (5′-ATGC-3′) site to a lesser extent.

Identification of the Oligonucleotide Termini Formed at the Site of Strand Scission. Gel electrophoretic analysis may be used to distinguish the termini obtained after strand cleavage by these complexes. Figure 3A,B illustrate the results of experiments in which Rh(phen)$_2$phi^{3+} and Rh(phi)$_2$bpy^{3+} were employed in reaction mixtures utilizing 3′- and [5′-^{32}P]-end-labeled oligonucleotide substrates. These reactions were examined by 20% polyacrylamide gel electrophoresis subsequent to treatment under neutral (control), alkaline, or reductive (NaBH$_4$) conditions. Figure 3A illustrates the products resulting from cleavage of the [3′-^{32}P]-end-labeled oligonucleotide indicating the exclusive formation of 5′-phosphate termini at the site of photocleavage, as evidenced by comigration with the products of Maxam–Gilbert sequencing reactions.[13] In comparison, an analysis of the products of the [5′-^{32}P]-end-labeled substrate (Figure 3B) indicates the formation of both 3′-phosphate termini and an additional product **1** which moves at a significantly slower rate relative to the 3′-phosphate terminus at each nucleotide step. While the formation of this slower moving product is apparent at each cleavage site after reaction with Rh(phi)$_2$bpy^{3+}, the secondary terminus is seen to a much smaller extent after reaction with Rh(phen)$_2$phi^{3+}. Figure 3B also shows the absence of 3′-phosphoglycolate termini, which would migrate at a faster rate than the 3′-phosphate termini.[3] Additional experiments (data not shown), where the samples were loaded directly onto the gels without heat denaturation, were carried out to search for the presence of any metastable intermediates as have been seen[2c] after cleavage with Cu(phen)$_2^{1+}$; no evidence of such intermediates was found. Photolysis in the presence of the rhodium complexes also results in the formation of a distinct band of radiolabeled material which migrates at a decreased rate relative to the unmodified oligonucleotide. Isolation of this material followed by atomic absorption

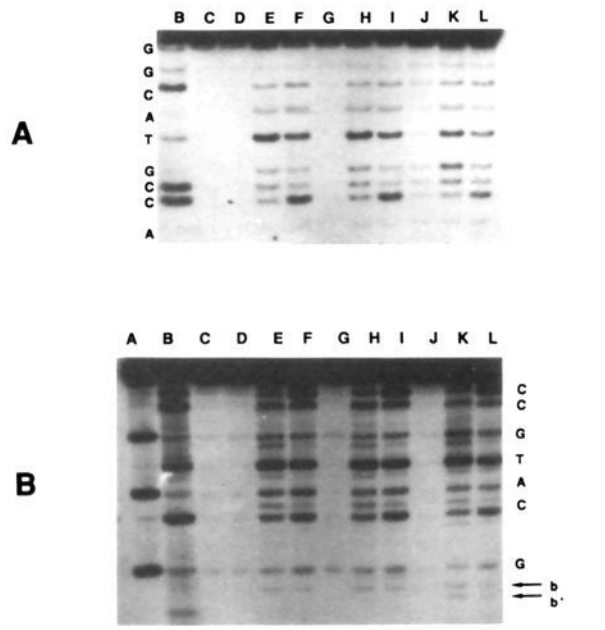

Figure 3. Comparison of $Rh(phen)_2phi^{3+}$ and $Rh(phi)_2phi^{3+}$ photocleavage of the oligonucleotide 5′-CTGGCATGCCAG-3′. A. Autoradiogram of 20% polyacrylamide gels of oligonucleotide labeled at the 3′-end. B. Autoradiogram of 20% polyacrylamide gels of oligonucleotide labeled at the 5′-end. Conditions for the cleavage reactions: 42 μM oligonucleotide, 25 μM Rh^{3+}, 50 mM sodium cacodylate, 7.5 min irradiation at 310 nm; lanes A and B, Maxam–Gilbert A + G and C + T reactions, respectively; lane C, oligonucleotide in the absence of irradiation; lane D, oligonucleotide irradiated in the absence of metal complex; lane E, oligonucleotide irradiated in the presence of $Rh(phi)_2bpy^{3+}$; lane F, oligonucleotide irradiated in the presence of $Rh(phen)_2phi^{3+}$; lanes G–I, reactions corresponding to lanes D–F followed by treatment with alkali (0.1 M NaOH, 60 °C, 2 min); lanes J–L, reactions corresponding to lanes D–F followed by treatment with reducing agent (0.1 M $NaBH_4$, 0 °C, 15 min). Note that in B ends marked b and b′ (lanes K and L) are assigned as the 3′-phosphoglycaldehyde terminus and the corresponding 3′-phosphoglycol terminus, respectively.

analysis indicated the presence of high levels of rhodium, suggesting that prolonged photolysis also promotes covalent binding.[16]

Following oligonucleotide cleavage, additional chemical modifications were carried out to characterize **1** further. To evaluate the extent of alkaline lability of the lesions formed, 5′- and [3′-^{32}P]-end-labeled reactions were treated with alkali (0.1 M NaOH, 60 °C, 2 min) prior to gel analysis (Figure 3B). This treatment yielded no additional strand scission. More stringent alkaline treatment (1 M piperidine, 90 °C, 30 min) of the reaction mixtures (data not shown) also had no effect on the extent of 5′- and 3′-phosphate termini produced, nor did such reaction alter the mobility or intensity of the unassigned slower moving end **1**. Figure 3B does show that reduction (0.1 M $NaBH_4$, 0 °C, 15 min) of the [5′-^{32}P]-end-labeled reaction mixtures prior to gel electrophoresis results in a slight increase in mobility of **1**; this is most readily apparent at the highly resolved 5′-G_3 site (Figure 3B). Similarly, harsher reduction (0.28 M $NaBH_4$, 25 °C, 90 min) of the [5′-^{32}P]-end-labeled reaction mixtures produced the same faster migration band, which was observed at each base site, and a concomitant diminution in the intensity of **1** (gel not shown). In comparison, $NaBH_4$ reduction of the [3′-^{32}P]-end-labeled substrate reaction mixtures (Figure 3A) had no effect on the mobility of the 5′-phosphate termini.

Effect of Oxygen Concentration on Oligonucleotide Product Formation. The effect of dioxygen concentration on the formation of the oligonucleotide products was examined in order to evaluate whether they were derived from aerobic or anaerobic pathways of degradation. $Rh(phi)_2bpy^{3+}$ induced photocleavage of [5′-^{32}P]-end-labeled oligonucleotide substrate was carried out under conditions of ambient, dioxygen purge, or argon saturation. This experiment demonstrated, as shown in Figure 4A, that DNA cleavage which leads to the 3′-phosphate terminus is independent of oxygen. However, the production of the secondary 3′-terminus **1** is clearly dependent upon the concentration of dioxygen. These results are quantitated in Table II.

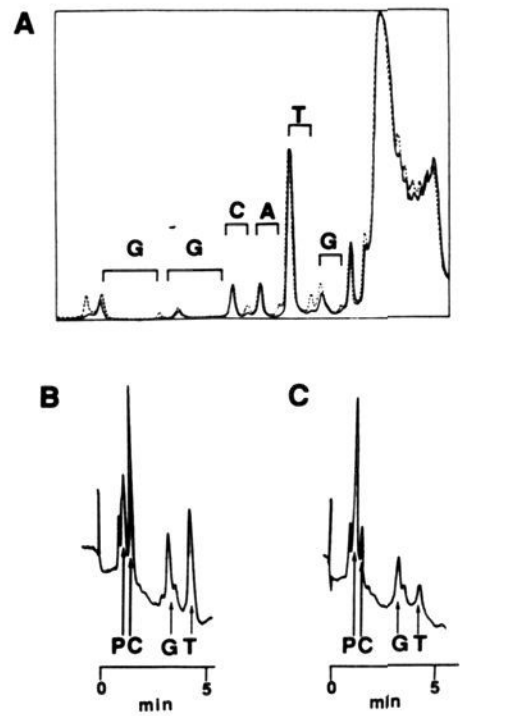

Figure 4. The effect of dioxygen on the production of putative 3′-aldehyde termini and base propenoic acids. A. Densitometric analysis of the 3′-termini detected through polyacrylamide gel electrophoresis of the photoreaction (310 nm, 7.5 min) of 42 μM oligonucleotide, 25 μM $Rh(phi)_2bpy^{3+}$, 50 mM sodium cacodylate under ambient concentrations of dioxygen (– –) and under conditions of argon saturation (—). The presence of dissolved dioxygen was minimized by saturating the reaction mixture with argon for 30 min prior to irradiation. The 3′-phosphate terminus at each labeled base site is associated with the slower moving 3′-phosphoglycaldehyde terminus. B. HPLC analysis showing the production of base-propenoic acids (P) under conditions of reduced oxygen concentration (argon saturation). C. HPLC analysis showing the production of base-propenoic acids (P) under ambient dioxygen conditions. Reaction conditions for B and C: 500 μM (in nucleotide) calf-thymus DNA, 25 μM $Rh(phi)_2bpy^{3+}$, 50 mM ammonium formate (elution buffer), 310 nm irradiation for 10 min.

Table II. Effect[a] of Oxygen Concentration on the 3′-Termini Produced in $Rh(phi)_2bpy^{3+}$-Induced Photocleavage Reaction of 5′-$C_1T_2G_3G_4C_5A_6T_7G_8C_9C_{10}A_{11}G_{12}$-3′

	experimental conditions					
	oxygen		ambient		argon	
	3′-P[b]	1[c]	3′-P	1	3′-P	1
G_3	1.6	0.6	1.7	0.4	1.6	0.1
G_4	0.6	0.2	0.9	0.2	0.8	0.2
C_5	2.3	1.4	2.8	1.3	2.2	0.6
A_6	2.2	1.2	2.5	1.0	2.2	0.0
T_7	11.8	2.3	13.0	1.5	13.0	0.6
G_8	3.7	1.1	3.4	0.9	2.3	0.4
total	**22.2**	**6.8**	**24.3**	**5.3**	**22.1**	**1.9**

[a] % yield of cleaved oligonucleotide. All numbers represent averages with deviations of ±5% of the densitometric quantification of three cleavage experiments and are normalized to the amount of undigested oligonucleotide. [b] Refers to the production of a 3′-phosphate terminus. [c] Refers to the production of the slower migrating terminus **1**.

(15) Campisi, D.; Morii, T.; Barton, J. K., unpublished results.

(16) Prolonged photolysis can yield $Rh(phen)(H_2O)_2^{3+}$ which in a secondary reaction can photobind to DNA. See, for example: Mahnken, R. E.; Bina, M.; Deibel, R. M.; Luebke, K.; Morrison, H. *Photochem. Photobiol.* **1989**, *49*, 519.

Table III. Quantitation of Products Formed by Rh(phen)$_2$phi^{3+}- and Rh(phi)$_2$bpy^{3+}-Induced Photocleavage[a] of 5′-CTGGCATGCCAG-3′

complex	base (μM)	oligonucleotide digest (μM)	nucleic acid base yield[b] (%)
Rh(phen)$_2$phi^{3+}	4.9	4.8	100
Rh(phi)$_2$bpy^{3+}	3.8	5.5	70

[a] Photocleavage reaction conditions for both complexes: 25 μM Rh, 42 μM oligonucleotide, 50 mM sodium cacodylate, 310-nm irradiation, 7.5 min. Analysis of products is described in the Experimental Section. [b] These values are based on oligonucleotide digested. The values represent averages of three experiments with deviations of <5%.

Identification and Quantitation of Monomeric Oligonucleotide Cleavage Products. Previous work[5] had indicated the formation of nucleic acid bases in DNA photoreactions mediated by the rhodium complexes. Presently, cleavage products formed upon interaction of Rh(phen)$_2$phi^{3+} or Rh(phi)$_2$bpy^{3+} with the substrate 5′-CTGGCATGCCAG-3′ were studied by HPLC in order to correlate quantitatively the extent of nucleic acid base release with the total amount of oligonucleotide strand scission. As shown in Table III, a 1:1 ratio of total nucleic acid base released to oligonucleotide digested is found in the Rh(phen)$_2$phi^{3+} induced photocleavage reactions. In comparison, Rh(phi)$_2$bpy^{3+}-induced photoreactions produced a 0.7:1 ratio of total nucleic acid base released to oligonucleotide digested. This finding suggests that approximately 30% of Rh(phi)$_2$bpy^{3+} photocleavage may produce another monomeric product. Moreover, densitometric quantitation (Table II) of the products observed by gel electrophoresis indicates that approximately 25% of the photocleavage mediated by Rh(phi)$_2$bpy^{3+} under ambient conditions produces the secondary 3′-terminus, **1**. These observations point to a nearly 1:1 correlation between the production of **1**, the formation of which is dependent on the dioxygen concentration of the reaction mixture, and of an alternate monomeric product.

Examination of oligonucleotide reaction mixtures after photocleavage by Rh(phi)$_2$bpy^{3+} using HPLC reveals a product in addition to nucleic acid bases. Identification of this degradation product was facilitated by HPLC analyses of product mixtures, as shown in Figure 5. Typical HPLC traces of the Rh(phi)$_2$bpy^{3+} and Rh(phen)$_2$phi^{3+} photoreactions show the release of nucleic acid base and a second product, **2** (labeled P in Figure 5). Clearly, **2** is produced to a greater extent in the Rh(phi)$_2$bpy^{3+} photoreaction than with Rh(phen)$_2$phi^{3+}. The product **2** shows a retention time substantially different from nucleic acid bases or authentic base propenals, which are formed in the Fe-bleomycin-mediated degradation of DNA.[3,4a] The formation of **2** was also examined as a function of dioxygen concentration. As shown in Figure 4B, this product diminishes in the absence of oxygen suggesting a correlation with the oxygen-dependent production of the 3′-terminus, **1**. The product **2** was collected and subjected to further photodegradation and reexamined by HPLC (Figure 5C). This analysis revealed degradation to free nucleic acid base. Mass spectral analysis of the collected peak (before photodegradation) indicates the presence of the ammonium salts of nucleic acid base propenoic acids of adenine, guanine, and cytosine (molecular ions 223, 234, and 199). Reduction of **2** was carried out with $NaBH_4/AlCl_3$, which was expected to reduce the acid to the corresponding alcohol,[17] was found to yield products which coelute with base propenols formed through the $NaBH_4$ reduction of the authentic base propenals (generated through Fe-bleomycin-mediated degradation of DNA). This result indicates the formation of a common product upon reduction of base propenals and **2**.

HPLC analysis of Rh(phi)$^{3+}$ reaction mixtures showed no evidence of nucleic acid base propenals in comparison to those formed in Fe-bleomycin-induced DNA degradation reactions. However, it was important to assess whether photolysis had led to photodegradation of base propenals, which may have been formed in the course of the cleavage reaction. Nucleic acid base propenals produced by Fe-bleomycin-induced degradation of DNA were found to be relatively stable under the conditions of UV irradiation used for the Rh(phi)$_2$bpy^{3+} and Rh(phen)$_2$phi^{3+} photoreactions. This observation verifies the lack of base propenal formation with DNA cleavage by Rh(phi)$^{3+}$ complexes. A summary of products obtained following photocleavage by the two rhodium complexes is given in Table IV.

(17) Brown, H. C.; Krishnamurthy, S. *Tetrahedron* **1967**, *35*, 567.

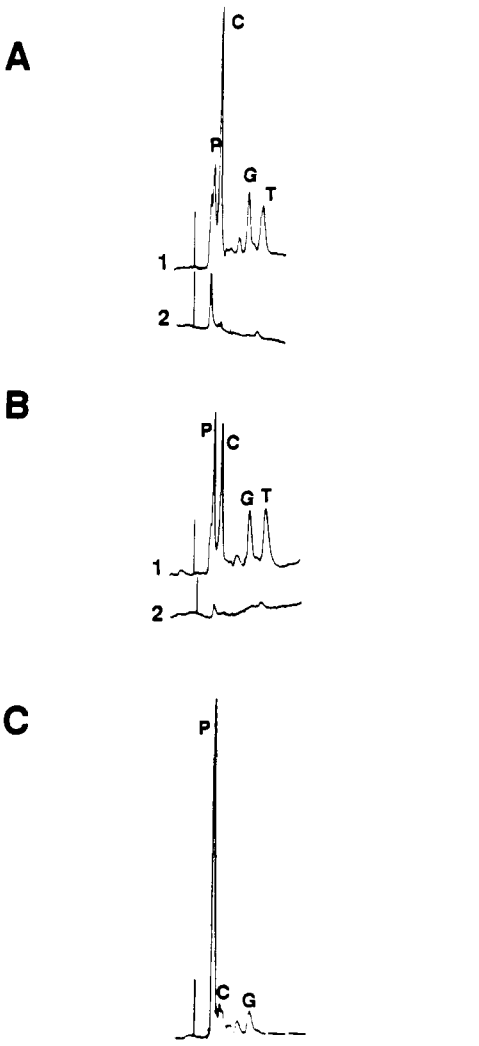

Figure 5. HPLC analysis of nucleic acid bases and base-propenoic acids produced with DNA degradation by Rh(phen)$_2$phi^{3+} and Rh(phi)$_2$bpy^{3+}. A. Analysis of products obtained after irradiation at 310 nm for 10 min of the reaction mixture in 50 mM ammonium formate containing Rh(phen)$_2$phi^{3+} (50 μM) in the presence (trace 1) or absence (trace 2) of 1 mM (in nucleotide) oligonucleotide. B. Analysis of products obtained after irradiation at 310 nm for 10 min of the reaction mixture in 50 mM ammonium formate containing Rh(phi)$_2$bpy^{3+} (50 μM) in the presence (trace 1) or absence (trace 2) of 1 mM (in nucleotide) oligonucleotide. C. HPLC analysis after further irradiation of the putative base propenoic acids. The putative base propenoic acids are marked P. C, G, and T refer to the nucleic acid bases cytosine, guanine, and thymine, respectively.

Table IV. Summary of Products Formed by Rh(phi)$_2$bpy^{3+}- and Rh(phen)$_2$phi^{3+}-Induced Photocleavage of 5′-CTGGCATGCCAG-3′

Rh(phi)$_2$bpy^{3+}	Rh(phen)$_2$phi^{3+}	oxygen dependence
5′- and 3′-phosphate termini	5′- and 3′-phosphate termini	−
3′-phosphoglycaldehyde termini		+
nucleic acid base	nucleic acid base	−
base propenoic acid		+

Discussion

Phi Complexes of Rhodium Bind to DNA by Intercalation. Phi complexes of rhodium avidly bind to double helical DNA. The

lower limit for affinity constants, estimated using a variety of techniques, is 10^7 M^{-1}. This high affinity is comparable to those found earlier for phi complexes of ruthenium.[12] These values are also quite comparable to, if not in excess of, affinity constants obtained for many organic dyes which intercalate into DNA.[14] Furthermore, several lines of evidence support an intercalative mode of association of the phi complexes with DNA.[18] Not only do the $Rh(phi)^{3+}$ complexes bind tightly to DNA, but as established through topoisomerase assays of helical unwinding, each bound complex promotes the unwinding of the DNA helix by approximately 20°. Besides promoting structural changes in the DNA helix, an electronic interaction between the complex and the DNA is readily observed through hypochromism and red shifts in absorbance maxima. NMR studies[19] of $Rh(phen)_2phi^{3+}$ bound to a decamer also are consistent with the phi ligand being bound rigidly between the base pairs.[20] Structurally, the phi ligand of these complexes provides a large aromatic surface area extended away from the metal center[11] through which to overlap, via intercalation, with the stacked Watson–Crick base pairs of the DNA helix. The increased aromatic surface of the phi ligand compared to phenanthroline results in an increase in the DNA binding constant of $Rh(phen)_2phi^{3+}$ versus $Rh(phen)_3^{3+}$ of several orders of magnitude.[12,22] These data, taken together, support intercalation of $Rh(phi)^{3+}$ complexes to DNA.

Recognition of DNA by Phi Complexes of Rhodium. The studies described here and earlier all point to intercalation of $Rh(phi)^{3+}$ complexes in the major groove of DNA. In particular $Rh(phen)_2phi^{3+}$ targets sites on restriction fragments[5] as well as on the Dickerson[23] dodecamer[7] which appear to be open in the major groove owing to propeller twisting or base pair tilting. Therefore, owing to its shape-selective recognition of the major groove, $Rh(phen)_2phi^{3+}$ has been used to map conformational variations in the 5S RNA gene, the binding site for the transcription factor TFIIIA.[9] Consistent with this targeting of the major groove has been the observation[8,24] that $Rh(phen)_2phi^{3+}$ does not recognize the deep and narrow major groove of double helical RNA. Instead $Rh(phi)^{3+}$ complexes target sites of tertiary interaction on tRNAs where, for example, three bases are hydrogen bonded one to another forming an accessible surface for stacking by the rhodium complex in the major groove. Therefore, like the metallointercalator $Pt(terpy)HET^+$ (terpy = 2,2′,2″-terpyridine, HET = 2-hydroxyethanethiolate),[25] $Rh(phi)^{3+}$ complexes appear to bind from the major groove through intercalation. $Rh(phi)^{3+}$ complexes should then be well positioned to abstract the C3′–H atom, which is located in the major groove.

Upon intercalation, both $Rh(phen)_2(phi)^{3+}$ and $Rh(phi)_2(bpy)^{3+}$ with photoactivation promote strand scission. However, their sites of reaction differ. The complexes, extremely similar to one another with respect to their electronic structure, show comparable quantum efficiencies for photoanation in the absence of DNA[11] and, as shown here, comparable quantum efficiencies for DNA strand scission. Therefore the intrinsic reactivity of each DNA site for photocleavage by the two complexes should be equal. The differences in DNA sites cleaved between the two complexes then must represent a difference in their recognition characteristics.

$Rh(phi)_2(bpy)^{3+}$ induces DNA strand scission in a predominantly sequence-neutral fashion, while $Rh(phen)_2(phi)^{3+}$ is observed to cleave only a subset of available sites. The strongest cleavage sites observed for $Rh(phen)_2(phi)^{3+}$ are those containing the consensus sequence 5′-py-*py*-pu-3′ such as 5′-CCAG-3′. Results indicate that 5′-CCAG-3′ sites are cleaved to an even greater extent at the 5′-*py*-pu-3′ step if the sequence is preceded by additional pyrimidines to the 5′-side. $Rh(phen)_2(phi)^{3+}$ also consistently recognizes homopyrimidine stretches of four or more base pairs. The recognition characteristics of $Rh(phen)_2phi^{3+}$ have been explained[5] based upon a consideration of structural features of the sequences targeted. X-ray crystallographic studies of oligonucleotides containing 5′-py-py-pu-3′ sites and homopyrimidine stretches all show openings in the major groove.[23] Owing to steric clashes between the overhanging phenanthrolines and the base-pair column upon intercalation of the phi ligand into the helix, some opening of the major groove would facilitate complex binding. For 5′-py-py-pu-3′ sites such openings may arise because of DNA propeller twisting. Previous studies indicate a correlation between enantioselective cleavage by $Rh(phen)_2phi^{3+}$ and the extent of differential propeller twisting at these sites.[7]

For $Rh(phi)_2bpy^{3+}$, however, no similar steric constraints appear to apply. The ancillary phi ligand is remarkably free of appendages which would normally clash with the base pair planes above and below the intercalation site; since the coordinated nitrogens on the ancillary phi ligand are primary imines, the only substituent on the nitrogen is a hydrogen atom. The shape of the complex therefore allows binding of $Rh(phi)_2bpy^{3+}$ at many sites along the DNA helix.

The structural basis for this difference in the site recognition characteristics of $Rh(phen)_2phi^{3+}$ and $Rh(phi)_2bpy^{3+}$ is illustrated in Figure 6. Here is shown a model for intercalation of each of the complexes into a base-pair step. Intercalation is shown in this model from the major groove of DNA. The results described here and elsewhere[5,7,8,9,24,25] all seem to support intercalation by metal complexes from the major groove. Remarkably, the differences in recognition characteristics of the two rhodium complexes may be understood based on the subtle differences in the shapes of these intercalators. These results underscore the importance of *shape-selection* in governing the recognition of a DNA site.

Phi Complexes of Rhodium Exhibit a 5′-Asymmetric Cleavage Pattern. Another prominent and novel characteristic of cleavage by $Rh(phen)phi^{3+}$ is the consistent 5′-shift in strand scission at a base pair site on one strand compared to the other. For $Rh(phi)_2bpy^{3+}$, this 5′-asymmetry is less evident owing to the greater sequence neutrality in cleavage of this rhodium complex. However this asymmetry can be observed at the preferred cleavage site 5′-A*T*GC-3′ on the oligonucleotide. According to a model derived by Dervan and co-workers,[26] an asymmetry in the cleavage pattern by a *diffusible* species will indicate whether the DNA cleavage agent is bound in the major or minor groove of the helix. A shift to the 3′-side was suggested as evidence for binding in the minor groove, while a shift to the 5′-side would indicate binding in the major groove. While this notion has been applied most to cleavage agents which produce a diffusible DNA oxidant,[2] it has also been invoked as evidence for minor groove binding by calicheamicin,[4b] an antitumor agent which cleaves DNA in a reaction yielding sharp bands, not unlike those seen with $Rh(phen)_2(phi)^{3+}$ and $Rh(phi)_2bpy^{3+}$. For both the rhodium complexes and calicheamicin the shift is 1–2 nucleotides, in contrast to the 5-nucleotide shift[2] seen with a diffusible oxidant. Since the $Rh(phi)^{3+}$ complexes show a 5′-asymmetry, this finding lends further support to the hypothesis that binding occurs from the major groove. Such a 5′-shift in the observed cleavage pattern is unprecedented and

(18) Long, E. C.; Barton, J. K. *Acc. Chem. Res.* **1990**, *23*, 271.
(19) David, S.; Barton, J. K., unpublished results.
(20) Also in support of the rigid orientation of these metallointercalators on DNA are emission polarization measurements[21] of $Ru(phen)_3^{2+}$ and $Ru(phen)_2dppz^{2+}$ (dppz = dipyridophenazine) bound to DNA, since these emissive analogues are structurally quite similar to $Rh(phen)_2phi^{3+}$.
(21) Friedman, A. E.; Kumar, C. V.; Turro, N. J.; Barton, J. K. *Nucl. Acids Res.* **1991**, *19*, 2595.
(22) Rehmann, J.; Barton, J. K. *Biochemistry* **1990**, *29*, 1701.
(23) (a) Heinemann, U.; Lauble, H.; Frank, R.; Blocker, H. *Nucl. Acids Res.* **1987**, *15*, 9531. (b) Dickerson, R.; Drew, H. R. *J. Mol. Biol.* **1981**, *149*, 761. (c) Hunter, W. N.; D'Estaintoto, D. L.; Kennard, O. *Biochemistry* **1989**, *28*, 2444. (d) Nelson, H. C. M.; Finch, J. T.; Luisi, B. F.; Klug, A. *Nature* **1987**, *330*, 221. (e) Coll, M.; Frederic, A.; Wang, A. H. J.; Rich, A. *Proc. Natl. Acad. Sci. U.S.A.* **1987**, *84*, 8385. (f) Timsit, Y.; Westhof, E.; Fuchs, R. P. P.; Moras, D. *Nature* **1989**, *341*, 459. (g) Wing, R.; Drew, H.; Takano, T.; Broka, C.; Tanaka, S.; Itakura, K.; Dickerson, R. E. *Nature* **1980**, *287*, 755. (h) Wang, A. H.-J.; Fujii, S.; van Boom, J. H.; Rich, A. *Proc. Natl. Acad. Sci. U.S.A.* **1982**, *79*, 3968. (i) Shakked, Z.; Rabinovich, D.; Cruse, W. T. B.; Egert, E.; Kennard, O.; Sala, G.; Salisbury, S. A.; Viswamitra, M. A. *Proc. R. Soc. London, B* **1981**, *231*, 479.
(24) Chow, C. S.; Behlen, L. S.; Uhlenbeck, O.; Barton, J. K. *Biochemistry* **1992**, *31*, 972.
(25) Wang, A. H. J.; Nathans, J.; van der Marel, G.; van Boom, J. H.; Rich, A. *Nature* **1978**, *276*, 471.
(26) Sluka, J. P.; Horvath, S. J.; Bruist, M. F.; Simon, M. I.; Dervan, P. B. *Science* **1987**, *238*, 1129.

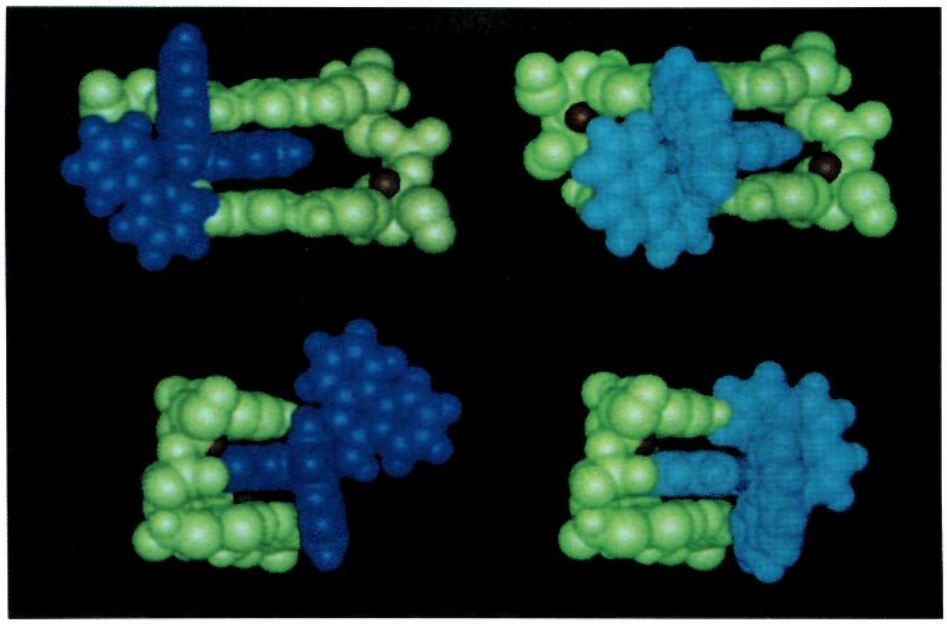

Figure 6. Models illustrating the intercalation of Rh(phi)$_2$bpy^{3+} (dark blue) and Rh(phen)$_2$phi^{3+} (aqua) through the phi into an unwound base pair step (green). The figure illustrates a model of how the shapes of Rh(phi)$_2$bpy^{3+} (left) and Rh(phen)$_2$phi^{3+} (right) may affect both their binding and cleavage chemistry. Above is a view showing intercalation into the major groove and below, the same model after 90° rotation, giving the side view of the complexes. The unhindered ancillary phi ligand of Rh(phi)$_2$bpy^{3+}, possibly owing to its hydrophobicity, allows this complex to slide to one side of the helix making the C-3′ hydrogen atom (marked in red) on the opposite strand more accessible to dioxygen. The side view emphasizes how the unhindered shape of Rh(phi)$_2$bpy^{3+} permits access into many local conformations along the DNA helix, while steric interactions of the ancillary phenanthrolines of Rh(phen)$_2$phi^{3+} are evident with base pairs above and below.

clearly provides information with regard to the orientation of the phi cleaving moiety relative to the DNA helix.

In addition to the 5′-asymmetric shift in cleavage patterns, the extent to which cleavage occurs on the 5′-side of the intercalation site is not identical on both strands, and this difference also provides information regarding the structures of the bound complexes. The differences in extent of cleavage on each strand is more clearly seen in the cleavage patterns of the dodecanucleotide 5′-CTGGCATGCCAG-3′. Here Rh(phen)$_2$phi^{3+} and Rh(phi)$_2$bpy^{3+} cleave most strongly at the 5′-C*C*AG-3′ and 5′-A*T*GC-3′ sites, respectively. The 5′-asymmetry indicates intercalation by Rh(phen)$_2$phi^{3+} at the CA step and by Rh(phi)$_2$bpy^{3+} at the TG step. Cleavage by Rh(phi)$_2$bpy^{3+} appears highly skewed toward one strand of the site as suggested by the 5-fold decrease in cleavage at the 5′-C_5 of the complementary strand. This observation suggests that the complex may be slid or canted to one side of the helix in the bound complex owing to hydrophobic interactions and/or steric considerations. Such interactions would lead to a complex which is oriented asymmetrically (toward one strand) in the site. In comparison, Rh(phen)$_2$phi^{3+} appears to cleave strongly at both the 5′-T_7 and the 5′-C_5 (5′-G*C*AT-3′; on the other strand) of the 5′-A*T*GC-3′ site, with only a slight preference for the 5′-T_7 (see Figure 3). This implies that, unlike Rh(phi)$_2$bpy^{3+}, Rh(phen)$_2$phi^{3+} is not significantly canted to one side of the helix; both the ancillary ligands in this complex are phenanthrolines. This asymmetry is also illustrated in our model in Figure 6.

Cleavage Products and Pathways of DNA Strand Scission. The characterization of photocleavage products has proved to be valuable in delineating aspects of the mechanism of strand scission by the Rh(phi)$^{3+}$ complexes. The production of sharp cleavage bands after the cleavage of restriction fragments or oligonucleotides suggests that the strand scission of DNA by rhodium complexes is not mediated by a diffusible oxidant. Rather, the cleavage appears primarily to involve a species which is generated and induces strand scission of the DNA backbone at precisely the position of binding. Rhodium polypyridyl complexes are known to be potent photooxidants; irradiation of the ligand transitions leads to ligand-to-metal-charge transfer (LMCT).[11,27] We have shown the quantum efficiencies for photoreaction by the phi complexes of rhodium to be comparable to those of Rh(phen)$_3^{3+}$ and that photolysis into a phi transition promotes preferential reaction of the phi ligand.[11] Therefore the active radical species responsible for DNA cleavage is likely to be the phi cation radical (either still coordinated or perhaps dissociated), formed as a result of LMCT and intimately bound to DNA. The positioning of the phi cation radical in the site can lead to the ready abstraction of a hydrogen from the deoxyribose ring. In experiments using specifically tritiated DNA the position of hydrogen atom abstraction has been confirmed.[28]

Our observation of nucleic acid bases released as a function of reaction indicate that the target of strand scission is the deoxyribose ring and not the heterocyclic aromatic base. Analysis of DNA degradation products resulting from photoreactions involving Rh(phen)$_2$phi^{3+} and Rh(phi)$_2$bpy^{3+} are not consistent with primary lesions at either the C1′-, C4′-, or C5′-positions of the deoxyribose. The products of reaction at each of these positions have been studied in detail.[2-4] Upon photocleavage with the rhodium complexes in the absence of oxygen, product analysis reveals the formation of 5′- and 3′-phosphate termini and the release of nucleic acid bases. Either with or without oxygen, no nucleic acid base propenals or phosphoglycolate termini were detected under conditions in which, given the extents of reaction, such products would have been readily apparent. However, in the presence of oxygen an additional 3′-terminus which migrates significantly slower than the corresponding 3′-phosphate product is apparent. This terminus is produced to a greater extent in the DNA photocleavage reaction with Rh(phi)$_2$bpy^{3+} than Rh(phen)$_2$phi^{3+}. The effects of alkali and of treatment with $NaBH_4$ confirm that the terminus is not a metastable species which decays

(27) (a) Chan, S.-F.; Chou, M.; Creutz, C.; Matsubara, T.; Sutin, N. *J. Am. Chem. Soc.* **1981**, *103*, 369. (b) Brown, G. M.; Chan, S.-F.; Creutz, C.; Schwartz, H. A.; Sutin, N. *J. Am. Chem. Soc.* **1979**, *101*, 7639. (c) Indelli, M. T.; Carioli, A.; Scandola, F. *J. Phys. Chem.* **1984**, *88*, 2685. (d) Ballardini, R.; Varani, G.; Balzani, V. *J. Am. Chem. Soc.* **1980**, *102*, 1719. (e) Frink, M. E.; Sprouse, S. D.; Goodwin, H. A.; Watts, R. J.; Ford, P. C. *Inorg. Chem.* **1988**, *27*, 1283.

(28) Long, E. C.; Absalon, M. J.; Stubbe, J. A.; Barton, J. K., manuscript in preparation.

ultimately to a 3′-phosphate. Neither the production of this 3′-terminus nor of the 3′- or 5′-phosphate termini are increased upon alkaline treatment. Alkaline lability in cleavage is commonly associated with lesions derived from C-1′ or C-4′ modification.[2-4,29] Finally, the lack of 3′-phosphoglycolate termini, the lack of an observable metastable intermediate, and the clear production of only a 5′-phosphate terminus are inconsistent with modification at the C4′-, C1′-, and C5′-deoxyribose positions, respectively.

We assign the slower migrating 3′-terminus **1** as a 3′-phosphoglycaldehyde. Treatment with $NaBH_4$ causes an increase in the mobility of the terminus. A 3′-phosphoglycaldehyde, under these conditions would be reduced to the corresponding, faster migrating alcohol. The DNA minor groove binding calicheamicin produces a modified deoxyribose fragment containing 5′-aldehyde ends which become reduced by $NaBH_4$ to produce faster moving 5′-alcohol ends.[4b] The possibility of an acidic functionality is ruled out because the addition of a negatively charged moiety would migrate faster, not slower as observed, than the corresponding phosphate end. It is noteworthy that in peroxide damaged *Escherichia coli* a stable 3′-phosphoglycaldehyde lesion has been characterized and found to migrate more slowly than the corresponding 3′-phosphate terminus using paper chromatography.[31] Importantly the formation of this phosphoglycaldehyde terminus upon cleavage by $Rh(phi)_2bpy^{3+}$ is correlated with the production of a base-propenoic acid. The comparison of the HPLC quantitation of nucleic acid base versus base-propenoic acid formation with the densitometric quantitation of 3′-phosphate and 3′-phosphoglycaldehyde termini shows excellent agreement between the extent of base-propenoic acid and the extent of 3′-phosphoglycaldehyde termini formed. Additionally, the 3′-phosphoglycaldehyde and base-propenoic acid are dependent upon the presence of dioxygen, while the production of phosphate termini and nucleic acid bases are not.

How can the photocleavage products obtained be reconciled with our model for binding of the phi complexes to the DNA helix? The lack of modification at the C1′-, 4′-, and 5′-positions of the deoxyribose ring is quite reasonable given the proposed structure shown in Figure 6 of the DNA-bound $Rh(phi)^{3+}$ complexes. A phi complex intercalated in the major groove of the DNA helix does not have direct access to these minor groove positions. However, the bound complex has ready access to the C3′–H of the deoxyribose ring. Indeed dinucleotide crystal structures of intercalation complexes[25] show alternating sugar puckering at an intercalation site, in which the C3′–H to the 5′-side of the intercalation site is pointed directly toward the intercalating moiety. This observation suggests one potential reason for the observed 5′-asymmetry in cleavage pattern. *Thus the most likely position for modification by the rhodium complexes is the C3′–H atom.*

Recently, the chemical products formed through oxygen-independent and -dependent pathways of strand scission involving the initial abstraction of the hydrogen from the C3′ position have been proposed.[3] It was predicted that in an oxygen-*independent* pathway abstraction of the C3′–H would result in the formation of nucleic acid bases and oligonucleotide termini containing 3′- and 5′-phosphates. Alternatively, an oxygen-*dependent* pathway would result in the formation of nucleotide base propenoic acids, 5′-phosphate termini, and 3′-phosphoglycaldehyde termini. Table IV summarizes the products obtained after reaction with $Rh(phen)_2phi^{3+}$ and $Rh(phi)_2bpy^{3+}$. The products found correspond to those predicted for radical formation at the C3′-position. $Rh(phen)_2phi^{3+}$ appears to promote degradation primarily through the oxygen-independent pathway, leading to the production of 3′- and 5′-phosphate termini and nucleic acid bases. For $Rh(phi)_2bpy^{3+}$ instead there is a partitioning between the oxygen-independent pathway and the oxygen-dependent pathway which leads to production of 3′-phosphoglycaldehyde termini, 5′-phosphates, and base-propenoic acids.

Scheme I summarizes the mechanism proposed.[3] Photolysis of either phi complex intercalated into DNA leads to abstraction of the C3′–H atom, with formation of the C3′-radical. Oxidation of the radical species, likely with Rh(II) as the oxidant,[31] and solvation of the resultant cation would lead, through a series of β-elimination steps, to the 5′-phosphate, 3′-phosphate, and nucleic acid base products observed. Alternatively, addition of dioxygen to the C3′-radical, followed by oxygen insertion into the C3′–C4′ bond and decomposition yields a 5′-phosphate and the correlated 3′-phosphoglycaldehyde terminus and base-propenoic acid. Furthermore, $Rh(phen)_2phi^{3+}$ has been shown to mediate the abstraction of the C3′–^{3}H of a tritiated polymer.[28]

The Shape-Selectivity in Reaction. The partitioning of the C3′-radical between oxygen-dependent and oxygen-independent pathways of decomposition clearly differs for $Rh(phen)_2phi^{3+}$ and $Rh(phi)_2bpy^{3+}$. $Rh(phi)_2bpy^{3+}$ photocleavage shows a greater level of reaction through the oxygen-dependent pathway than does $Rh(phen)_2phi^{3+}$. This difference may also be understood based upon our models for their binding to the helix and also explained through the differences in the *shapes* of these complexes. The binding by $Rh(phi)_2bpy^{3+}$ occurs at all sites since the ancillary phi ligand is pulled back from the intercalating phi ligand; this disposition of the ancillary phi also permits access of dioxygen to the C3′-position. In the case of $Rh(phen)_2phi^{3+}$, the bulky ancillary phenanthroline ligands not only preclude binding at closed sites but also shelter the C3′-position from addition of dioxygen. Furthermore, canting of $Rh(phi)_2bpy^{3+}$ toward one strand of the helix appears to increase the accessibility for dioxygen to the complementary strand at the site of intercalation. Consistent with this notion, we observe that oligonucleotide cleavage with $Rh(phi)_2bpy^{3+}$ at the T_7 of the strong 5′-$A_6T_7G_8C_9$-3′ site is associated with a large extent of 3′-phosphoglycaldehyde formed at the C_5 of the complementary strand. It appears therefore that $Rh(phi)_2bpy^{3+}$ promotes both pathways of strand degradation from the C-3′ radical intermediate while $Rh(phen)_2phi^{3+}$ disfavors the utilization of dioxygen in DNA strand scission.

These observations suggest that the overall shape of the $Rh(phi)^{3+}$ complexes not only dictates DNA recognition but also determines the outcome of DNA cleavage. The reaction *and* the site-recognition are shape-selective. These results illustrate the intimate relationship between recognition and reactive characteristics of molecules bound selectively to DNA.[32] In designing mimics of DNA-binding proteins and natural products, and in constructing wholly original designs for sequence-specific cleaving agents, there has been much focus on the separation of binding and cleaving domains. In the case of the transition metal complexes that we have designed, a clear separation between binding and cleaving functionalities is inappropriate. Such an intimate relationship between recognition and reaction of DNA-binding molecules may be more general and important to consider in understanding the reactions of DNA-binding proteins and small molecules.

Acknowledgment. We are grateful to the NIH (GM33309 to J.K.B., National Research Service Training Award to A.M.P., GM07216) for their financial support. E.C.L. is a Fellow of the Jane Coffin Childs Memorial Fund for Medical Research. We are also grateful to Dr. T. Morii and Dr. J. Stubbe for helpful discussions.

(29) (a) Kappen, L. S.; Chen, I.-H.; Goldberg, I. H. *Biochemistry* **1988**, *27*, 4331. (b) Kappen, L. S.; Goldberg, I. H. *Biochemistry* **1989**, *28*, 1027.
(30) Demple, B.; Johnson, A.; Fung, D. *Proc. Natl. Acad. Sci. U.S.A.* **1986**, *83*, 7731.
(31) Mulazzani, Q. G.; Emmi, S.; Hoffman, M. Z.; Venturi, M. *J. Am. Chem. Soc.* **1981**, *103*, 3362.
(32) Two examples illustrating this relationship have been seen with bleomycin. See, for example: Long, E. C.; Hecht, S. M.; van der Marel, G. A.; van Boom, J. H. *J. Am. Chem. Soc.* **1990**, *112*, 5272. Carter, B. C.; Murty, V. S.; Reddy, K. S.; Wang, S. N.; Hecht, S. M. *J. Biol. Chem.* **1990**, *256*, 4193.